Article

FACE
1–8

DOI: 10.1177/27325016231177456
journals.sagepub.com/home/fac
Sage

Nasal Airflow Dynamics Before and After Septorhinoplasty for Correction of Cleft Lip Nasal Deformity: A Single Patient Case Report

Raluca E. Gosman[1], Jeffrey R. Marcus[1], and Dennis O. Frank-Ito[1]

Abstract

Background: Unilateral cleft lip nasal deformity (uCLND) creates multiple sites of nasal airway obstruction, impacting patients' quality of life. Surgical restoration of function remains technically challenging and complex.

Objectives: This is a single patient case report to determine consistency of patient's subjective perception of nasal outcomes after septorhinoplasty with objective assessments, and effectiveness of standard surgical techniques in targeting sites of greatest nasal anatomical obstruction.

Method: Patient-reported quality of life (QOL) measures were collected. Pre- and post-surgery radiographic images of a patient with uCLND were obtained for computational fluid dynamics (CFD) modeling of patient-specific nasal function. Objective assessments were obtained using rhinomanometry and CFD. CFD-derived localized resistance at multiple cross-sectional segments were determined and used to identify greatest nasal obstructive sites.

Results: Patient-reported QOL scores improved by 20 to 73 points. CFD-calculated bilateral resistance decreased from 0.155 to 0.061 Pa.s/ml, cleft-side resistance from 0.407 to 0.091 Pa.s/ml, and non-cleft-side from 0.228 to 0.120 Pa.s/ml. Rhinomanometry showed similar decreases in resistance. On the cleft side, 25 identified sites of greatest obstruction decreased to 15 sites post-surgery; on the non-cleft side, 23 sites of greatest obstruction decreased to 16 sites post-surgery.

Conclusion: Results suggest improvement in nasal patency after septorhinoplasty. Additional greatest obstructive sites in the post-surgical airway were mostly around the superior airway.

Keywords

septorhinoplasty, computational fluid dynamics, outcomes

Introduction

In their 2002 paper, Shih and Sykes[1] noted that correction of the cleft-lip nasal deformity (CLND) is a difficult task requiring the facial plastic surgeon to have a comprehensive understanding of the complex anatomic abnormalities present in patients with CLND. Standard septorhinoplasty in skeletally mature patients with CLND involves septoplasty performed at the anterior (caudal) portion of the septum.[2-4] For patients characterized with unilateral CLND (uCLND), which is of particular importance in the present study, the nasal septum is deviated on both sides of the nasal cavity: the septum is deviated to the non-cleft side at the anterior portion, and deviated to the cleft side posteriorly.[1,5,6] The anterior portion of the septum is mainly cartilaginous and the middle to posterior portion of the septum is comprised almost entirely of bone.[2] Friel et al[2] reported that there is a significant degree of deviation at the middle to posterior portion of the septum. This unrepaired middle to posterior deviation accounts for about 75% of the maximal degree of septal deviation within the nasal cavity.[2] Unlike anterior cartilaginous septoplasty, middle to posterior bony septoplasty is technically challenging and complicated to perform because of the risks involved in bony resection, such as mucosal tears, post-surgery bleeding, and cerebrospinal fluid leak.[2,3]

Blair and Brown[7] in 1932 first described the implication of cleft lip and/or palate on nasal function, yet 90 years later,

[1]Duke University Medical Center, Durham, NC, USA

Corresponding Author:
Dennis O. Frank-Ito, Department of Head and Neck Surgery & Communication Sciences, Duke University Medical Center, 40 Duke Medicine Circle, DUMC Box 3805, Durham, NC 27710, USA.
Email: dennis.frank@duke.edu

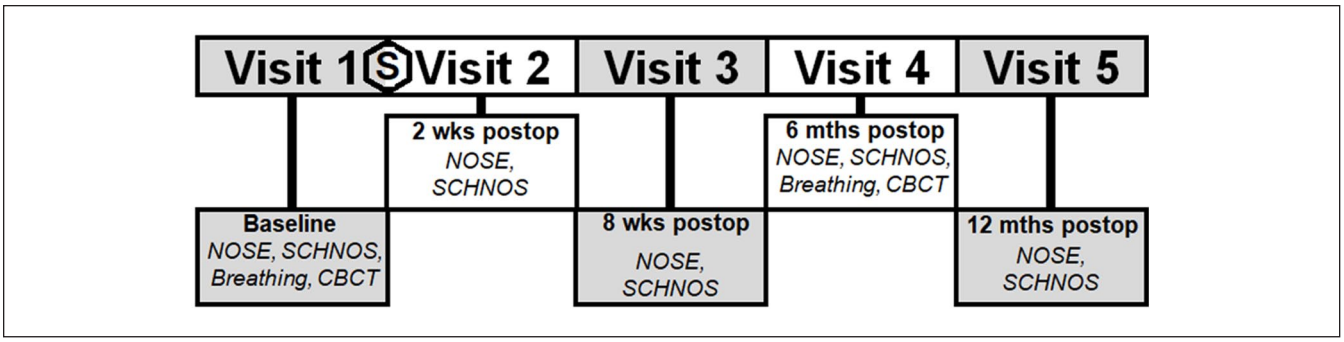

Figure 1. Patient study timeline from Visit 1 to Visit 5. The "S" between Visits 1 and 2 denotes that surgery was performed between these 2 visits.

the status quo remains largely unchanged as it pertains to progress on the appropriate interventions necessary to restore nasal function to normative levels in patients with CLND.[2,3,8-10] The sad reality is that despite nasal breathing difficulty and associated reduced quality of life experienced by patients with CLND, reported severity of symptoms of nasal airway obstruction are underreported because patients are more aware and troubled by the stigma of their facial appearance and the corresponding influence on their psychosocial well-being. According to findings in the literature, severity of obstructive breathing in patients with CLND is reported to be 20% to 30% higher than those of the general population.[2,3,8-10] Furthermore, Warren et al[11] reported that about 70% of cleft individuals have impaired functional nasal breathing and that upward of 80% "mouth-breathe," which in turn results in a common complaint of dry mouth after sleeping. Between 13% and 40% of cleft individuals also report some trouble breathing during exercise.[9]

Commonly used patient-reported outcome measures for evaluating cleft-induced nasal airway obstruction in patients with CLND include the Nasal Obstruction Symptom Evaluation (NOSE) survey,[12] CLEFT-Q,[13] and the Standardized Cosmesis and Health Nasal Outcomes Survey (SCHNOS) survey.[14] In a 2016 study by Sobol et al,[9] NOSE scores from 176 pediatric patients with cleft lip and/or cleft palate and 333 controls revealed that symptoms of nasal airway obstruction were more frequently reported among patients with cleft lip and/or cleft palate. In another study using the NOSE survey to evaluate nasal outcomes before and after secondary rhinoplasty for definitive repairs of cleft-induced nasal airway obstruction, it was found that patients with CLND reported significant improvement in nasal patency postoperatively.[15] This finding is in agreement with a recently published longitudinal study by Carlson et al,[16] which shows significant improvement in NOSE scores after secondary cleft rhinoplasty for correction of nasal airway obstruction in patients with cleft lip and/or palate.

Prior works by our group have involved the use of photogrammetry and anatomically realistic patient-specific computational models to (1) characterize the unilateral septal and dorsal deformities in patients with uCLND[17]; (2) compare differences in nasal obstruction experience by patients with uCLND and noncleft patients with clinical diagnosis of nasal obstruction[18]; and (3) identify anatomic sites of greatest nasal obstruction in patients with uCLND and using virtual surgical methods to assess the effects of different surgical procedures on nasal patency.[19] In general, the structural abnormalities present in patients with uCLND create multiple sites of nasal airway obstruction.[2-4] While the majority of the cleft lip and/or palate studies that have addressed nasal airway obstructive symptoms have focused on comparison with normal subjects and/or among different cleft phenotypes,[2-6,8-10,20-23] only a handful of publications have focused on the effectiveness of current surgical interventions in improving patients' nasal function. For this reason, the objective of this research study is to investigate surgical outcomes in a patient with uCLND who underwent surgery for definitive cleft repairs of nasal airway obstruction using clinical measures and computational fluid dynamics (CFD) modeling.

Materials and Methods

Patient

A 21-year-old female patient with uCLND was prospectively recruited for this study that is funded by the National Institute of Dental & Craniofacial Research of the National Institutes of Health and approved by the Duke University Health System Institutional Review Board for Clinical Investigations. Inclusion criteria included: (1) clinical diagnosis of uCLND; (2) has not had cleft rhinoplasty or septoplasty for correction nasal airway obstruction; (3) elects to have surgery for nasal airway obstruction and give written informed consent; and (4) elects to undergo cone beam computed tomography (CBCT) scanning before and at 4 to 11 months after nasal surgery.

Patient Assessments

As depicted in Figure 1, the patient had a total of 5 visits: Visit 1 (baseline); Visit 2 (2 weeks after surgery); Visit 3

(8 weeks after surgery); Visit 4 (6 months after surgery); and Visit 5 (12 months after surgery). The following assessments were performed during each or some of the visits: (1) Patient-reported Nasal Obstruction Symptom Evaluation (NOSE) survey[12]; (2) Patient-reported Standardized Cosmesis and Health Nasal Outcomes Survey (SCHNOS) survey[14]; (3) Anterior rhinomanometry breathing measurement evaluated at the standard (75 Pa) level using the NR6 Clinical/Research Rhinomanometer (GM Instruments Ltd, Kilwinning, Scotland, U.K); and (4) Patient radiographic images from CBCT scans.

During Visit 1, the preoperative baseline visit, patient-reported NOSE and SCHNOS were administered followed by breathing measurement and CBCT scanning. Day of surgery took place between Visits 1 and 2, and the patient underwent external approach septorhinoplasty for definitive repairs of cleft-induced nasal airway obstruction. This procedure included septal reconstruction with bone and soft tissue work at the caudal and dorsal septum; an osteotomy was made on the cleft side of the nasal floor to eliminate a maxillary spur, and the deviated perpendicular plate was resected. Bilateral inferior turbinate reduction was also completed, as well as nasal tip reconstruction. The internal nasal valve was repaired using septal cartilage and a spreader flap technique on the concave side, and the external nasal valve was repaired using a lateral crural strut graft and mucosal Z-plasty.

The patient was seen 2 weeks after surgery for Visit 2 follow-up assessments, which included administering of patient-reported NOSE and SCHNOS surveys. Similarly, Visit 3 follow-up assessments were identical to Visit 2. For Visit 4, in addition to patient-reported NOSE and SCHNOS surveys, postoperative breathing measurement and CBCT scanning were performed. Final patient assessments were performed during Visit 5 with administration of patient-reported NOSE and SCHNOS surveys.

In brief, NOSE and SCHNOS are validated patient-reported outcome questionnaires used to assess patient subjective perception of (1) nasal function and (2) nasal cosmesis. The NOSE scale consists of 5 items relating to nasal congestion, blockage, difficulty breathing, trouble sleeping, and air hunger sensation.[12] SCHNOS consists of 2 separate domains such that the first 4 items pertain to nasal obstruction (SCHNOS-O), while the final 6 items involve nasal cosmesis (SCHNOS-C).[14]

Computational Fluid Dynamics (CFD) Modeling

Before and after surgery, radiographic images of the patient obtained from CBCT scans were read into the imaging analysis software Avizo 3D 2021.1 (Thermo Fisher Scientific, Waltham, Massachusetts, USA) for creation of anatomically realistic and patient-specific three-dimensional nasal cavity models. These models were segmented, with subsequent manual editing as needed, similar to previously published models.[17-19,24-26] To specify the direction of inspiratory airflow in the nasal cavity models and prepare the models for airflow simulations, reconstructed nasal cavity models were imported into ICEM-CFDTM 2021 R2 (ANSYS, Canonsburg, Pennsylvania, USA) for creation of a box covering the external soft-tissue nose to represent inlet where ambient air flows into the nasal cavity. An outlet plane was also created at the end of the nasopharynx to represent location where air exited the nasal cavity.

To solve the discretized governing equations necessary for simulating nasal airflow, hybrid polyhedral-prism meshes were generated in the before (396 000 cells) and after (410 000 cells) surgery patient-specific nasal cavity models using Fluent™ Meshing 2021 R2 (ANSYS, Canonsburg, Pennsylvania, USA). Three near wall prism layers were created with an initial prism layer aspect ratio of 6 and prism layers growth rate set to 1.2. Following mesh generation, steady-state, laminar inspiratory airflow was simulated in the patient's before and after surgery nasal cavity models using Fluent™ Solution 2021 R2 to mimic patient-specific physiological inhalation airflow rate. Fluent™ Solution 2021 R2 uses the finite volume method to numerically solve the conservation of mass and momentum governing equations for laminar viscous, and incompressible flow; defined as

$$\nabla.\vec{u} = 0 \quad \rho\left(\vec{u}.\nabla\right)\vec{u} = -\nabla p + \mu\nabla^2\vec{u}$$

where $\vec{u} = \vec{u}\left(x, y, z\right)$ is velocity vector field, $\rho = 1.204$ kg/m^3 is fluid density, $\mu = 1.825\times10^{-5}\,\mathrm{kg/m-s}$ is dynamic viscosity, and p is pressure. The "mass flow outlet" boundary condition was specified at the outlet to target resting inspiration of 0.0003 kg/s (15 L/min). Atmospheric conditions were specified at the inlet (box) with 0-gauge pressure. No-slip boundary conditions was specified along the walls (nasal mucosa), and the walls were assumed to be stationary.

Nasal resistance was calculated as $\Delta P/Q$(Pa/s/ml) where ΔP was bilateral/unilateral pressure drop from nostril(s) to choana, and Q is bilateral/unilateral volumetric flow rate.

Identification of Greatest Obstructive Sites

We used the method described in Tillis et al[19] to determine effectiveness of surgery in targeting sites of greatest nasal obstruction for correction. For the respective before and after surgery nasal cavity models, sites of greatest nasal obstruction in each unilateral airway were determined by creating a grid-like structure with 15 equally spaced cross sections between the posterior nasal alar rim (CS-01) to choana (CS-15), and then dividing each cross section into superior, middle, and inferior segments. This resulted in 45 total segments for each unilateral nasal passage (15 cross sections times 3 each for superior, middle, and inferior). Next, airflow resistance was calculated at each unilateral segment. Lastly, a segment was considered a site of greatest obstruction if the resistance at that segment was greater than 3 times

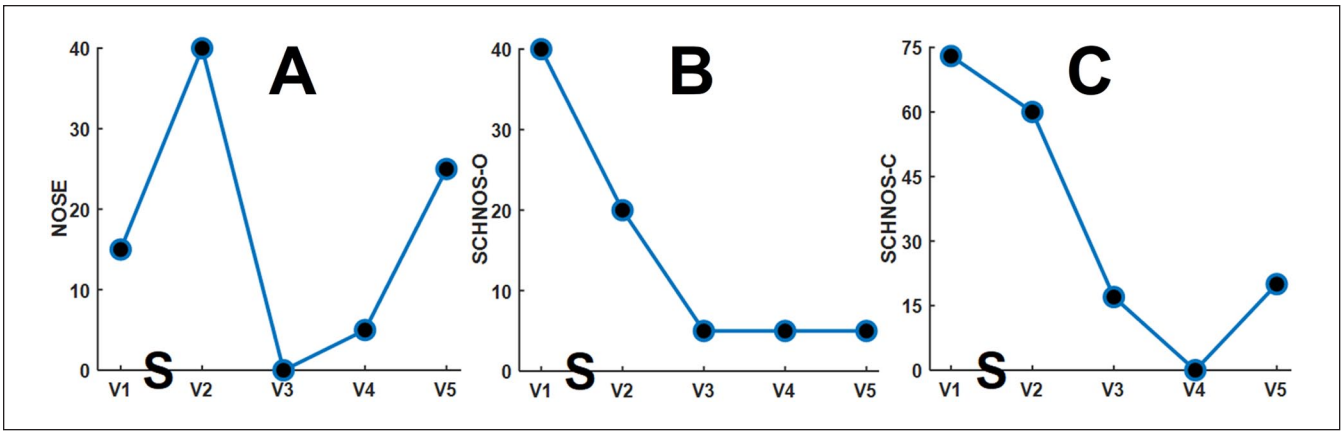

Figure 2. (A) Visit 1 (V1) to Visit 5 (V5) NOSE Scores; (B) Visit 1 (V1) to Visit 5 (V5) SCHNOS-O scores; and (C) Visit 1 (V1) to Visit 5 (V5) SCHNOS-C scores. NOSE = Nasal Obstruction Symptom Evaluation; SCHNOS-O = Standardized Cosmesis and Health Nasal Outcomes Survey Nasal Obstruction domain; SCHNOS-C = Standardized Cosmesis and Health Nasal Outcomes Survey Nasal Cosmesis domain. The "S" between Visits 1 and 2 denotes that surgery was performed between these 2 visits.

preoperative unilateral nasal resistance on the nasal side containing that segment.[19]

Results

Patient-Reported Outcomes

Figure 2A shows the patient's NOSE scores from Visit 1 (preoperative baseline) to Visit 5 (12 months postoperative). The "S" on the *x*-axis between Visit 1 and Visit 2 in Figure 2A denotes that surgery was performed between the 2 visits. At baseline visit (Visit 1), patient's NOSE score was 15, with a highest NOSE score of 40 during Visit 2 (2 weeks after surgery). At 12 months, the patient reported a NOSE score of 25 (Visit 5), which was 10 points higher than her preoperative baseline score during Visit 1. On the contrary (Figure 2B), patient-reported SCHNOS-O scores were highest (40) during Visit 1 and declined to 5 by Visit 3 through the final 12 months postoperative visit (Visit 5). With regards to nasal cosmesis (Figure 2C), SCHNOS-C was highest (73) at Visit 1, dropped to 0 by Visit 4, and increased to 20 by Visit 5.

Inspiratory Flow Analysis

The patient's left side is the cleft side. During Visit 1, preoperative rhinomanometry measurement could not be completely on the cleft side since the patient was severely obstructed on that side and was unable to complete the respiratory cycle necessary for measurement to be obtained. Thus, the cleft side was termed "maximally obstructed." Preoperative rhinomanometry measurement of nasal resistance on the non-cleft side (right side) was 16.67 Pa.s/ml. Postoperative rhinomanometry measurement was done on Visit 4; nasal resistance values were 2.28 (cleft side) and 1.40 Pa.s/ml (non-cleft side).

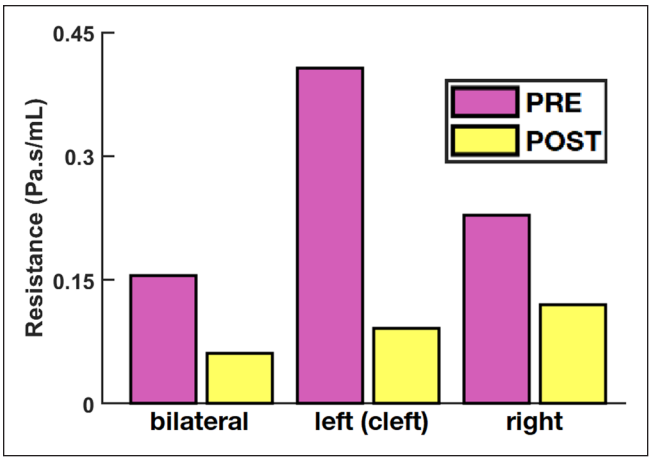

Figure 3. Computational fluid dynamics modeling (CFD)-generated bilateral and unilateral nasal airway resistance pre- and post-surgery.

Post-operative rhinomanometric values were above normal limits for unilateral airway resistance.[27-30]

Bar plots in Figure 3 represent CFD-computed nasal resistance before (Visit 1) and after (Visit 4) surgery. In general, nasal resistance decreased after surgery. Bilateral nasal resistance values were: preoperative = 0.155 versus postoperative = 0.061 Pa.s/ml, a 61% reduction in bilateral nasal resistance after surgery. Nasal resistance values on the cleft side (left) were preoperative = 0.407 Pa.s/ml versus postoperative = 0.091 Pa.s/ml, and on the non-cleft side (right) were preoperative = 0.228 Pa.s/ml versus postoperative = 0.120 Pa.s/ml. Nasal resistance decreased by 78% and 47% on the cleft and non-cleft sides, respectively, and resulted in values within normal limits for unilateral resistance.[27-30]

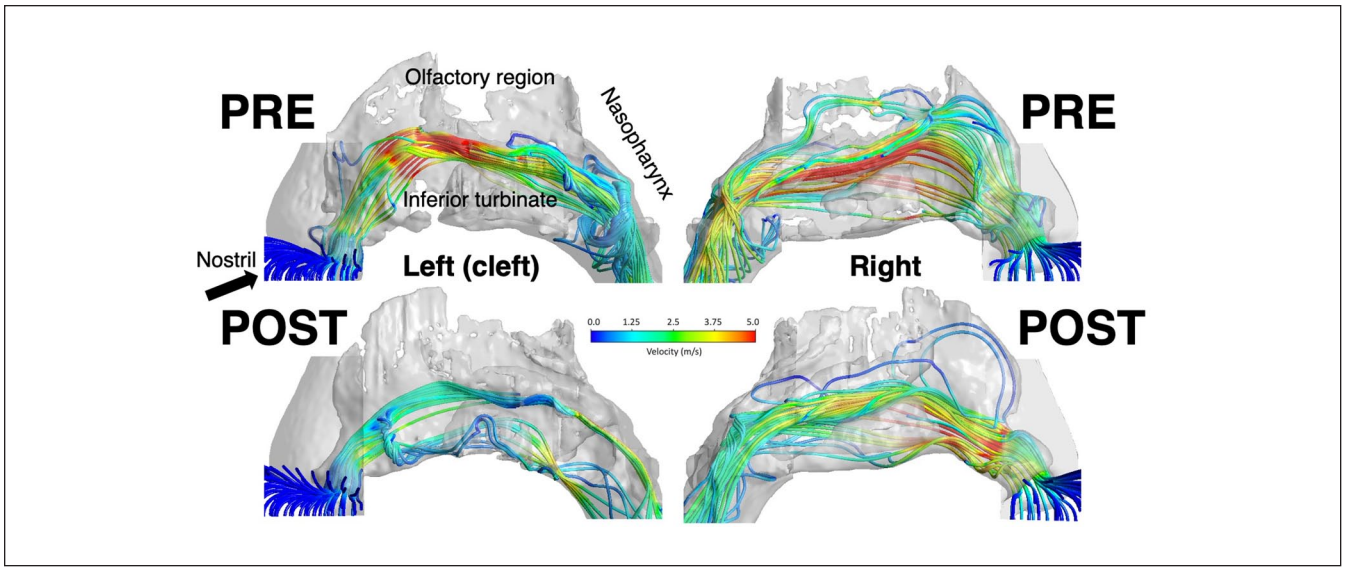

Figure 4. Pre- and post-surgery airflow streamlines in the left and right nasal cavities. Views are from the lateral aspect, with gray areas representing a transparent, three-dimensional airspace. Streamlines are shown colored from slower velocities in blue to faster velocities in red. Airflow was simulated from the inlet (nostril) to the outlet (choana).

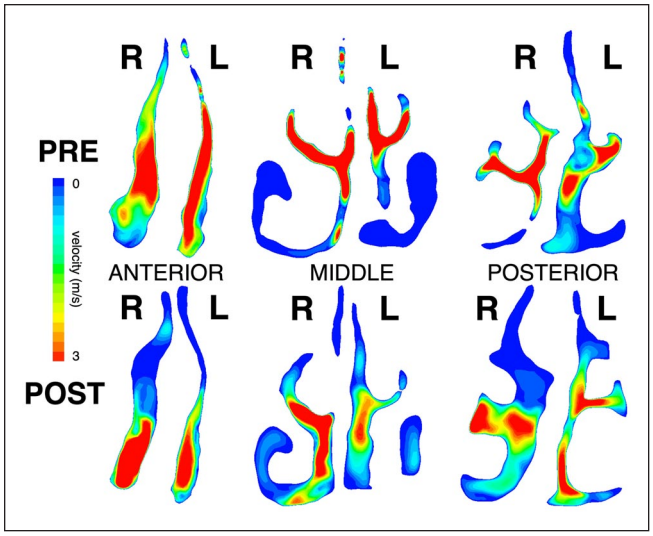

Figure 5. Pre- and post-surgery airflow speeds within 3 cross sections (anterior, middle, and posterior) of the bilateral nasal airspace. Slower velocities are seen in blue, and faster velocities are seen in red. The left side is the cleft side.

Airflow and Velocity Profile

Figure 4 shows spatial airflow visualization pattern from CFD simulations in the before and after surgery nasal cavity models, computed from 100 streamlines colored by velocity magnitude. Before surgery, airflow mainly transverses through the middle region on the cleft side (left) and spreads over more regions on the non-cleft side while avoiding occluded regions around the superior and the inferior airspace. After surgery, the airflow pattern on the cleft side was predominately in the middle and inferior regions. With the exception of a few superior airflow streamlines, flow pattern on the non-cleft side was not vastly different compared to the cleft side.

Figure 5 shows velocity contours of airflow at 3 cross sections in the nasal cavity: anterior, middle, and posterior. The fastest flow profiles in the before surgery anterior cross section were around the middle to inferior on the cleft side (L) and around the middle region on the non-cleft side (R). At the middle and posterior cross sections, fastest flow before surgery occurred around the middle meatus on the cleft and non-cleft sides. After surgery, airflow was fastest at all 3 cross sections around the middle to inferior regions for both cleft and non-cleft sides.

Sites of Greatest Obstruction

The 15 cross sections shown in Figure 6 are delineated into inferior, middle, and superior segments; thus, each unilateral nasal cavity contained 45 segments. On the preoperative cleft side (left), median (min, max) resistance values (Pa/s/ml) at these segments were: Inferior median = 8.865 (min = 0.186, max = 215.39); Middle = 0.418 (0.254, 0.622); and Superior = 5.082 (1.202, 39.567). These segments' resistance values were compared with 3 times the preoperative cleft side (left) unilateral resistance value ($3 \times 0.407 = 1.221$) to determine greatest obstructive sites. There were 11 identified sites of greatest nasal obstruction in the inferior region of the preoperative cleft side (left), 0 identified sites in the middle region, and 14 identified sites in the superior airway (25 total).

On the preoperative non-cleft side (right), the segments' median (min, max) resistance values (Pa/s/ml) were: Inferior median = 1.2191 (min = 0.104, max = 2.110); Middle = 0.241 (0.128, 0.306); and Superior = 3.765 (0.367, 56 992). These

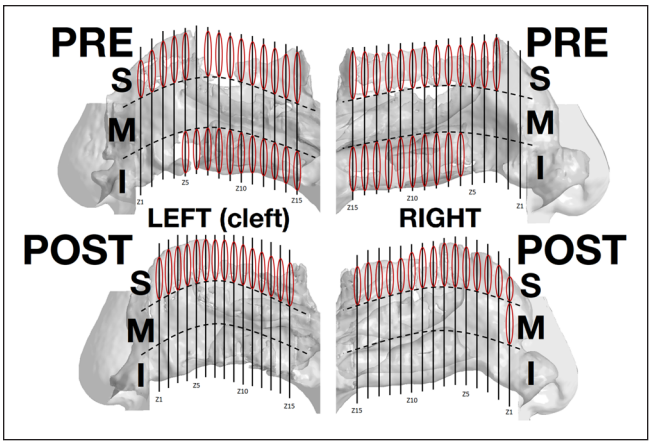

Figure 6. Sites of greatest obstruction pre- and post-surgery in the left and right nasal cavities. Views are from the lateral aspect, with gray areas representing a transparent, three-dimensional airspace. Vertical solid lines are numbered Z1 to Z15 from anterior to posterior to delineate 15 equally spaced coronal crosssections. Horizontal dashed lines represent the splitting of a unilateral cross-section into superior (S), middle (M), and inferior (I) segments. Red circles show local regions of obstruction.

resistance values were compared with 3 times the preoperative non-cleft side (right) unilateral resistance value ($3 \times 0.228 = 0.684$). Thus, 10 sites of greatest obstruction were identified in the inferior airway, 0 in the middle region, and 13 superiorly (23 total).

Postoperatively, cleft side (left) median (min, max) resistance values (Pa/s/ml) were: Inferior median = 0.187 (min = 0.090, max = 0.606); Middle = 0.159 (0.010, 0.372); and Superior = 3.912 (1.386, 10.464). These resistance values were compared with 3 times the preoperative cleft side unilateral resistance, resulting in 0 identified sites of greatest obstruction in the middle and inferior regions and 15 identified sites in the superior airway (15 total).

Segments' median (min, max) resistance values (Pa/s/ml) on the postoperative non-cleft side were: Inferior median = 0.247 (min = 0.0122, max = 0.348); Middle = 0.264 (0.183, 0.964); and Superior = 63.51 (2.58, 593 810). After comparing these resistance values with 3 times the preoperative non-cleft side unilateral resistance, the number of identified sites of greatest obstruction were 0 (inferior), 1 (middle), and 15 (superior) (16 total).

Discussion

In most clinical settings, the evaluation of nasal obstruction often relies solely on patient-reported symptoms and physician examination.[31,32] As evidenced by the patient presented in this study, reliance on patients' subjective perception of postoperative nasal patency can sometimes be very difficult. Although NOSE scores and SCHNOS-O scores have been reported to be strongly correlated (correlation coefficient = .943, $P < .001$),[14] there was little agreement between the NOSE and SCHNOS-O scores in our patient from Visit 1 to Visit 5. By Visit 2, 2 weeks after surgery, the patient reported a worsened NOSE score of 25 points from baseline (Visit 1) and an improved SCHNOS-O score of 20 points from baseline. From Visit 3 (8 weeks after surgery) to Visit 5 (12 months after surgery), the patient-reported NOSE scores ranging from a 15-point improvement (Visit 3) to a 10-point worsening (Visit 5). During the same period, the patient's SCHNOS-O scores demonstrated a consistent 35-point improvement. Whereas the patient's NOSE did not indicate a minimal clinically important difference across visits, SCHNOS-O did indicate a minimal clinically important difference across visits.[33]

The discordant NOSE and SCHNOS-O scores from Visit 1 to Visit 5 reinforces the notion that patients with uCLND may not reliably describe symptoms of nasal obstruction as a significant impairment, especially if considered in comparison to improved esthetic outcomes. These patients have had symptoms of nasal obstruction their whole life, and they may not reliably report their symptoms in comparison to patients with normal noses who secondarily develop obstruction.[4] As is the case with the patient investigated in the present study, with regards to patients with uCLND, it is often difficult to make a clear determination whether or not surgery does relieve patient-reported obstructive symptoms.[34] For instance, it has been reported that up to 70% of individuals with treated uCLND for nasal obstruction continue to have impaired nasal breathing.[11] Furthermore, among this patient population, persistent obstructive symptoms is a common source of patient dissatisfaction after surgery.[35]

The present study highlights a major limitation of anterior rhinomanometry to measure unilateral flow rate and nasal resistance. At the baseline visit, we assessed the patient's cleft side (left) to be maximally obstructed since the patient was severely obstructed on this side and was unable to tolerate the rhinomanometer when attempting to breathe solely on the cleft side with the non-cleft (right) plugged. After a few seconds of attempting to measure unilateral flow and resistance on the cleft side, we had to discontinue as the patient was showing visible signs of distress trying. Nonetheless, the patient's unilateral and bilateral flow rate and nasal resistance were calculated using CFD modeling. The undeniable power of CFD modeling has been utilized by our group for over a decade to provide highly important insights into identification of specific variables that correlate with patient-reported symptoms of nasal obstruction[36-39]; race and gender differences on nasal respiratory physiology[25,40-42]; and analyzing the nasal function of patients with uCLND.[17-19,43]

Airflow streamlines in Figure 4 depict patent regions of the nasal airway with dominant airflow access before and after surgery. Notice that the regions where nasal airflow had easy access corresponded to anatomical sites that were not identified as greatest obstructive sites in Figure 6. In particular, before surgery, airflow mostly shunted through the middle region of the nasal airway on the cleft side and through the middle and anterior-superior region on the non-cleft side.

These regions were not identified as anatomical sites of greatest obstruction. Similar airflow behavior was observed in the airway after surgery. Conversely, the superior airway region was identified as anatomical sites of greatest obstruction in the before and after surgery nasal models. Surgery is not usually performed superiorly because of the complexity and increased risk of damaging the olfactory nerves. In a recent study by our group, Tillis et al[19] used information from anatomical sites of greatest nasal obstruction to determine virtual surgery procedures that specifically targeted the correction of these obstructive regions.

Conclusions

A major limitation of this study is that it is a single patient study. This project is currently ongoing and future work will involve multiple patients. In conclusion, uCLND-induced nasal obstruction is a complicated condition to characterize and treat. Clinical modalities for evaluation such as rhinomanometry or patient-reported questionnaires may not provide a comprehensive understanding of the nature of uCLND pathophysiology. CFD modeling provided detailed objective assessment of the before and after surgery nasal airways, changes in nasal patency after surgery, and anatomical sites of greatest obstruction.

Declaration of Conflicting Interests

The author(s) declared no potential conflicts of interest with respect to the research, authorship, and/or publication of this article.

Funding

The author(s) disclosed receipt of the following financial support for the research, authorship, and/or publication of this article: This research was supported by the National Institute of Dental & Craniofacial Research of the National Institutes of Health under Award Number R01DE028554. The content is solely the responsibility of the authors and does not necessarily represent the official views of the National Institutes of Health.

Ethical Approval

This study is approved by the Duke University Health System Institutional Review Board under protocol number Pro00102005.

ORCID iD

Raluca E. Gosman https://orcid.org/0000-0002-9608-2025

References

1. Shih CW, Sykes JM. Correction of the cleft-lip nasal deformity. *Facial Plast Surg*. 2002;*18*(4):253-262.
2. Friel MT, Starbuck JM, Ghoneima AM, et al. Airway obstruction and the unilateral cleft lip and palate deformity: contributions by the bony septum. *Ann Plast Surg*. 2015;*75*(1):37-43.
3. Massie JP, Runyan CM, Stern MJ, et al. Nasal septal anatomy in skeletally mature patients with cleft lip and palate. *JAMA Facial Plast Surg*. 2016;*18*:347-353.
4. Fisher MD, Fisher DM, Marcus JR. Correction of the cleft nasal deformity: from infancy to maturity. *Clin Plast Surg*. 2014;*41*(2):283-299.
5. Latham RA. The pathogenesis of the skeletal deformity associated with unilateral cleft lip and palate. *Cleft Palate J*. 1969;*6*:404-414.
6. Crockett D, Bumstead R. Nasal airway, otologic and audiologic problems associated with cleft lip and palate. In: Bardach J, Morris HL, eds. *Multidisciplinary Management of Cleft Lip and Palate*. WB Saunders; 1990: 672.
7. Blair VP, Brown JB. Nasal abnormalities, fancied and real: the reaction of the patient: their attempted correction. *Int J Orthod Oral Surg Radiography*. 1932;*18*(4):363-401.
8. Drake AF, Davis JU, Warren DW. Nasal airway size in cleft and noncleft children. *Laryngoscope*. 1993;*103*(8):915-917.
9. Sobol DL, Allori AC, Carlson AR, et al. Nasal airway dysfunction in children with cleft lip and cleft palate: results of a cross-sectional population-based study, with anatomical and surgical considerations. *Plast Reconstr Surg*. 2016;*138*(6):1275-1285.
10. Warren DW, Hairfield WM, Dalston ET, Sidman JD, Pillsbury HC. Effects of cleft lip and palate on the nasal airway in children. *Arch Otolaryngol Head Neck Surg*. 1988;*114*(9):987-992.
11. Warren DW, Drake AF, Davis JU. Nasal airway in breathing and speech. *Cleft Palate Craniofac J*. 1992;*29*(6):511-519.
12. Stewart MG, Smith TL, Weaver EM, et al. Outcomes after nasal septoplasty: results from the nasal obstruction septoplasty effectiveness (NOSE) study. *Otolaryngol Head Neck Surg*. 2004;*130*(3):283-290. doi:10.1016/j.otohns.2003.12.004
13. Wong KW, Forrest CR, Goodacre TE, Klassen AF. Measuring outcomes in craniofacial and pediatric plastic surgery. *Clin Plast Surg*. 2013;*40*(2):305-312.
14. Moubayed SP, Ioannidis JPA, Saltychev M, Most SP. The 10-item standardized cosmesis and Health Nasal Outcomes Survey (SCHNOS) for functional and cosmetic rhinoplasty. *JAMA Facial Plast Surg*. 2018;*20*(1):37-42.
15. Chaithanyaa N, Rai KK, Shivakumar HR, Upasi A. Evaluation of the outcome of secondary rhinoplasty in cleft lip and palate patients. *J Plast Reconstr Aesthet Surg*. 2011;*64*(1):27-33.
16. Carlson AR, Kosyk MS, Zapatero ZD, et al. A longitudinal study of improvement in nasal airway obstruction after secondary cleft rhinoplasty. *Plast Reconstr Surg*. 2023;*151*(2):385-394.
17. Marcus JR, Brown DA, Carpenter D, Glener A, Allori A, Frank-Ito D. Multimodal characterization of the mature septal deformity and airspace associated with unilateral cleft lip and palate. *Plast Reconstr Surg*. 2019;*143*(3):865-873.
18. Frank-Ito DO, Carpenter DJ, Cheng T, et al. Computational analysis of the mature unilateral cleft lip nasal deformity on nasal patency. *Plast Reconstr Surg*. 2019;*7*(5):e2244.
19. Tillis RT, Shah R, Martin HL, Allori AC, Marcus JR, Frank-Ito DO. A systematic analysis of surgical interventions for the airway in the mature unilateral cleft lip nasal deformity: a single case study. *Int J Comput Assist Radiol Surg*. 2022;*17*(1):41-53. doi:10.1007/s11548-021-02396-z
20. Morén S, Mani M, Lundberg K, Holmström M. Nasal symptoms and clinical findings in adult patients treated for unilateral cleft lip and palate. *J Plast Surg Hand Surg*. 2013;*47*(5):383-389.
21. Farzal Z, Walsh J, Lopes de Rezende Barbosa G, et al. Volumetric nasal cavity analysis in children with unilateral and

bilateral cleft lip and palate. *Laryngoscope*. 2016;*126*:1475-1480.
22. Trindade IE, Gomes Ade O, Fernandes Mde B, Trindade SH, Silva Filho OG. Nasal airway dimensions of children with repaired unilateral cleft lip and palate. *Cleft Palate Craniofac J*. 2015;*52*(5):512-516.
23. Grossmann N, Brin I, Aizenbud D, Sichel J-Y, Gross-Isseroff R, Steiner J. Nasal airflow and olfactory function after the repair of cleft palate (with and without cleft lip). *Oral Surg Oral Med Oral Pathol Oral Radiol Endod*. 2005;*100*(5):539-544.
24. Sicard RM, Shah R, Frank-Ito DO. Analyses on the influence of normal nasal morphological variations on odorant transport to the olfactory cleft. *Inhal Toxicol*. 2022;*34*:350-358.
25. Shah R, Frank-Ito DO. The role of normal nasal morphological variations from race and gender differences on respiratory physiology. *Respir Physiol Neurobiol*. 2022;*297*:103823.
26. Sicard RM, Frank-Ito DO. Role of nasal vestibule morphological variations on olfactory airflow dynamics. *Clin Biomech*. 2021;*82*:105282.
27. Zhao K, Jiang J. What is normal nasal airflow? A computational study of 22 healthy adults. *Int Forum Allergy Rhinol*. 2014;*4*(6):435-446. doi:10.1002/alr.21319
28. Moore EJ, Kern EB. Atrophic rhinitis: a review of 242 cases. *Am J Rhinol*. 2001;*15*(6):355-361.
29. Eccles R. Nasal airflow in health and disease. *Acta Otolaryngol*. 2000;*120*(5):580-595. doi:10.1080/000164800750000388
30. Warren DW, Walker JC, Drake AF, Lutz RW. Assessing the effects of odorants on nasal airway size and breathing. *Physiol Behav*. 1992;*51*(2):425-430. doi:10.1016/0031-9384(92)90161-t
31. Recker C, Hamilton Gs, 3rd. Evaluation of the patient with nasal obstruction. *Facial Plast Surg*. 2016;*32*(1):3-8. doi:10.1055/s-0035-1570502
32. Keeler J, Most SP. Measuring nasal obstruction. *Facial Plast Surg Clin North Am*. 2016;*24*(3):315-322. doi:10.1016/j.fsc.2016.03.008
33. Kandathil CK, Saltychev M, Abdelwahab M, Spataro EA, Moubayed SP, Most SP. Minimal clinically important difference of the standardized cosmesis and health nasal outcomes survey. *Aesthet Surg J*. 2019;*39*(8):837-840.
34. Tsang CLN, Nguyen T, Sivesind T, Cervin A. Long-term patient-related outcome measures of septoplasty: a systematic review. *Eur Arch Otorhinolaryngol*. 2018;*275*(5):1039-1048. doi:10.1007/s00405-018-4874-y
35. Sharif-Askary B, Carlson AR, Van Noord MG, Marcus JR. Incidence of postoperative adverse events after Rhinoplasty: A Systematic Review. *Plast Reconstr Surg*. 2020;*145*(3):669-684. doi:10.1097/prs.0000000000006561
36. Kimbell JS, Frank DO, Laud P, Garcia GJ, Rhee JS. Changes in nasal airflow and heat transfer correlate with symptom improvement after surgery for nasal obstruction. *J Biomech*. 2013;*46*(15):2634-2643. doi:10.1016/j.jbiomech.2013.08.007
37. Kimbell JS, Garcia GJM, Frank DO, Cannon DE, Pawar SS, Rhee JS. Computed nasal resistance compared with patient-reported symptoms in surgically treated nasal airway passages: a preliminary report. *Am J Rhinol Allergy*. 2012;*26*(3):94-98. doi:10.2500/ajra.2012.26.3766
38. Sullivan CD, Garcia GJ, Frank-Ito DO, Kimbell JS, Rhee JS, Frank-Ito DO. Perception of better nasal patency correlates with increased mucosal cooling after surgery for nasal obstruction. *Otolaryngol Head Neck Surg*. 2014;*150*(1):139-147. doi:10.1177/0194599813509776
39. Frank-Ito DO, Garcia G. Clinical implications of nasal airflow simulations. In: Inthavong K, Singh N, Wong E, Tu J, eds. *Clinical and biomedical engineering in the human nose: A Computational Fluid Dynamics Approach, Springer*. 2021;157-192.
40. Keeler JA, Patki A, Woodard CR, Frank-Ito DO. A computational study of nasal spray deposition pattern in four ethnic groups. *J Aerosol Med Pulm Drug Deliv*. 2016;*29*(2):153-166. doi:10.1089/jamp.2014.1205
41. Patki A, Frank-Ito DO. Characterizing human nasal airflow physiologic variables by nasal index. *Respir Physiol Neurobiol*. 2016;*232*:66-74.
42. Russel SM, Frank-Ito DO. Gender differences in nasal anatomy and function among Caucasians. *Facial Plast Surg Aesthet Med*. 2023;*25*:145-152. doi:10.1089/fpsam.2022.0049
43. Li H, Martin HL, Marcus JR, Frank-Ito DO. Analysis of nasal air conditioning in subjects with unilateral cleft lip nasal deformity. *Respir Physiol Neurobiol*. 2021;*291*:103694.